Elucidating the mechanism of substrate recognition by the bacterial Hsp90 molecular chaperone

Timothy O. Street[3], **Xiaohui Zeng**[6], **Riccardo Pellarin**[4], **Massimiliano Bonomi**[4], **Andrej Sali**[4], **Mark J.S. Kelly**[5], **Feixia Chu**[6], and **David A. Agard**[1,2]

[1]Department of Biochemistry & Biophysics, University of California, San Francisco, CA 94158, USA

[2]Howard Hughes Medical Institute, University of California, San Francisco, CA 94158, USA

[3]Department of Biochemistry, Brandeis University, Waltham MA 02453, USA

[4]Department of Bioengineering and Therapeutic Sciences, University of California, San Francisco, CA 94158, USA

[5]Department of Pharmaceutical Chemistry, University of California, San Francisco, CA 94158, USA

[6]Department of Molecular, Cellular, & Biomedical Sciences, University of New Hampshire, Durham, New Hampshire 03824

Abstract

Hsp90 is a conformationally dynamic molecular chaperone known to promote the folding and activation of a broad array of protein substrates ("clients"). Hsp90 is believed to preferentially interact with partially folded substrates, and it has been hypothesized that the chaperone can significantly alter substrate structure as a mechanism to alter the substrate functional state. However, critically testing the mechanism of substrate recognition and remodeling by Hsp90 has been challenging. Using a partially folded protein as a model system, we find that the bacterial Hsp90 adapts its conformation to the substrate, forming a binding site that spans the middle and C-terminal domains of the chaperone. Crosslinking and NMR measurements indicate that Hsp90 binds to a large partially-folded region of the substrate and significantly alters both its local and long-range structure. These findings implicate Hsp90's conformational dynamics in its ability to bind and remodel partially folded proteins. Moreover, native-state hydrogen exchange indicates that Hsp90 can also interact with partially folded states only transiently populated from within a thermodynamically stable native state ensemble. These results suggest a general mechanism by which Hsp90 can recognize and remodel native proteins by binding and remodeling partially folded states that are transiently sampled from within the native ensemble.

Corresponding author: Timothy Street – tstreet@brandeis.edu, (781)-736-4961.

Introduction

A large network of highly conserved molecular chaperones protects cells against protein misfolding and aggregation. Given the diversity of the proteome, different molecular chaperones have evolved to stabilize initial or late events in protein folding as well as to help recover from thermal or other proteotoxic stresses. For example, some chaperones (*e.g.* Hsp60, Hsp70, Hsp104) use nucleotide binding and hydrolysis to drive conformational changes that modulate chaperone affinity for nascent polypeptides or largely unfolded protein substrates. Other chaperones work independently of nucleotide but can populate different assembly states (*e.g.* small heat shock proteins [1]) or undergo conformational changes from differing conditions, such as the redox environment (*e.g.* Hsp33 [2]) or low pH (*e.g.* HdeA [3]). Despite their abundance, the detailed mechanisms of many of these chaperones are only poorly understood.

Hsp90 is a ubiquitous nucleotide-dependent molecular chaperone. The Hsp90 dimer is composed of three stable domains (N-terminal; NTD, Middle domain; MD, C-terminal; CTD). Nucleotide binding occurs at the NTD and dimerization occurs at the CTD. The apo state of Hsp90 is highly flexible, where a weak interface between the MD/CTD (Fig 1) creates a wide range of open extended states [4; 5]. Addition of non-hydrolyzable ATP results in a closed state wherein the two arms make contact at the NTD (Figure 1 [6]), organizing the catalytic machinery for ATP hydrolysis. In addition, a transiently populated highly compact state has been observed by electron microscopy under ADP conditions [7]. Hsp90 has a slow rate of ATP hydrolysis, indicating that a large energetic barrier governs the chaperone activity. Although both ATPase and a common set of conformational states have been observed for Hsp90 homologs ranging from bacteria (HtpG) to human [8; 9; 10; 11], the absolute rates and conformational equilibria are species-specific [7]. Despite these significant advances, little is known about the relationship of Hsp90's conformational dynamics to its function as a chaperone.

Among its many functions in the cell, Hsp90 can facilitate kinase activation and nuclear receptor ligand binding by a currently unknown mechanism [12]. This modulation of native activity has suggested that Hsp90 can interact with non-native states of substrates that are late in their folding pathway. Furthermore, the ability of Hsp90 to facilitate protein-protein or protein-ligand interactions suggests that the chaperone can actively influence the conformation of bound substrates, which could alter the substrate folding process and subsequent functional outcome. Unfortunately, because partially folded states are typically sparingly populated and aggregation-prone, exploring the Hsp90 mechanism in biochemical and biophysical detail has proven very challenging. A second complication is that eukaryotic cytosolic Hsp90s typically work in collaboration with a host of cochaperones that serve to modulate the Hsp90 ATPase cycle and aid substrate binding and release. As a result, little is known about how Hsp90 recognizes specific structural states of its substrates, or how the chaperone affects substrate structure and folding.

To alleviate many of the practical limitations of Hsp90/substrate studies, we have focused on a minimal system using the *E. coli* Hsp90 homolog, $Hsp90_{Ec}$ (HtpG), which lacks the numerous co-chaperones and post-translational modifications found in eukaryotic Hsp90s,

and have combined this with a well-studied, NMR-tractable partially folded model substrate, Δ131Δ. This truncation variant of Staphylococcal Nuclease (SN) is non-aggregating, compact [13], and retains some local native-like structure [14; 15]. NMR order parameters [16] suggest a locally formed hydrophobic core within residues ~70–120. The presence of residual structure within Δ131Δ suggested that it could be a suitable model system to determine how Hsp90 can recognize structural features beyond short unstructured regions of polypeptide.

Previous work demonstrated that Δ131Δ binds to Hsp90$_{Ec}$, shifts the conformation of apo from an extended conformation to a V-shape, and activates its ATPase. By contrast, Δ131Δ that is refolded via a tight binding inhibitor fails to interact [17]. Moreover, Hsp90$_{Ec}$ binds to the most structured region of Δ131Δ, around residues 80–115, indicating a very different strategy than Hsp70, which recognizes very short and fully unfolded protein regions. Although these findings established a basic phenomenology of an Hsp90/substrate interaction, because binding was mapped by the localized loss of HSQC peaks, the underlying mechanism and structural consequences of Δ131Δ recognition remained obscure. Furthermore, these findings did not indicate whether Hsp90 could interact with thermodynamically stable proteins that have already undergone nascent folding and thus only rarely sample non-native states.

A combination of SAXS and NMR was used to identify a Δ131Δ binding region on the MD towards the base of the Hsp90$_{Ec}$ dimer cleft [18]. More recently, the same region was identified in an *E. coli* genetic screen for Hsp90$_{Ec}$-defective mutations, and then extended to the adjacent region of the CTD [19]. Altogether, eight Hsp90$_{Ec}$ mutations at the MD/CTD significantly disrupt Δ131Δ binding (Figure 1). These mutation sites cluster in the apo-state crystal structure, whereas on small angle X-ray scattering (SAXS) models of the dominant fully open conformation [4], the sites are distended and disorganized (Figure 1). These results suggest a mode of molecular recognition in which the chaperone utilizes its conformational flexibility to position hydrophobic regions on the MD/CTD into a continuous surface. Importantly, the same region was shown to be functionally relevant for client activation by yeast Hsp90 [19], attesting to conserved underlying mechanisms for Hsp90s from prokaryotes to eukaryotes.

Here we build on this previous work to elucidate the mechanism of Hsp90/substrate recognition and determine how the chaperone affects the structure and folding of its target protein. We find that Hsp90's flexibility at the MD/CTD is critical for binding Δ131Δ and that a minimal construct of the MD/CTD is sufficient to bind a large partially folded region of Δ131Δ. Using chemical crosslinking and mass-spectrometry along with computational modeling of the data, we show that the interactions between Hsp90 and Δ131Δ result in significant local and long-range structural changes within the substrate. Finally, using native-state hydrogen exchange we discover that Hsp90 can interact with partially folded states of SN that are only transiently populated under folding conditions. Together these findings provide the basis of a structural mechanism by which Hsp90 can alter the functional outcome of substrates by binding and remodeling partially folded states that are transiently sampled from the native ensemble.

Results

The positioning of   131   binding sites on Hsp90 (Figure 1), immediately suggests a recognition mechanism in which Hsp90's flexibility around the MD/CTD is critical for binding. To test this idea we investigated whether disrupting the MD/CTD interface affects substrate binding. Previous work identified a pH-dependent conformational change in Hsp90$_{Ec}$ controlled by histidine 446 buried between the MD/CTD [5]. At neutral pH the wild-type Hsp90$_{Ec}$ adopts an equilibrium between a fully extended and a partially closed state (similar to the Grp94 crystal structure [20]). At higher pH the fully open conformation is favored, and at lower pH the Grp94 conformation is favored [5]. The H446E mutation pushes the equilibrium to the fully open state, which can still progress to the closed ATP state. If MD/CTD reconfiguration is required for substrate recognition then the H446E mutation should reduce substrate binding and any associated chaperone conformational changes.

The effect of H446E on   131   binding was assessed by fluorescence polarization anisotropy [17]. Although residue 446 is not located at the known   131   binding site (Figure 2A, see red spheres in inset), the H446E mutation effectively abrogates binding (Figure 2A, blue squares). In addition, we used SAXS to assess whether   131   could alter the conformation of H446E as it does with wild-type Hsp90$_{Ec}$, shown schematically in the Figure 2B inset [17]. The P(r) curve, which summarizes the inter-atomic scattering distances within Hsp90$_{Ec}$, shows how   131   binding to wild type Hsp90$_{Ec}$ (Figure 2B, dashed lines) reduces the scattering probability at long distances (>100 Å) and increases the probability of intermediate distances. By contrast, the H446E mutation adopts a fully extended conformation as described previously [5], and, importantly, its conformation is unaffected by   131   (Figure 2B, solid lines). These measurements support a recognition mechanism in which structural reconfiguration at the MD/CTD is necessary for binding substrate. Next we sought to investigate whether the MD/CTD region is sufficient for binding   131 .

Previous NMR measurements indicated that Hsp90$_{Ec}$ interacts with a highly structured region of   131   (residues ~80–115 [17]). However the large size of the Hsp90$_{Ec}$ dimer (140 kD), and potential conformational changes within this region resulted in complete disappearance of HSQC peaks around the binding region on   131 , which precluded a more detailed description of the binding interaction. Given that a continuous MD/CTD surface is required for optimal   131   binding, we explored whether a monomeric MD/CTD fragment lacking the CTD dimerization helix (residues 383–604; referred to as MC) would allow detailed interactions to be addressed by NMR via chemical shift mapping.

In contrast to the peak losses observed previously, it is now evident that addition of MC causes chemical shifts in ^{15}N-labeled   131   (Figure 3A). The binding interaction is in intermediate exchange with increasing MC concentrations resulting in an initially small peak movement with broadening, and a subsequent appearance of a new peak (a detailed example is shown in Supplemental Figure 1A). Some residues, such as V104, show multiple chemical shifts, suggesting modest local conformational heterogeneity. To ensure that these chemical shifts were the result of specific interactions we measured the   131   HSQC in the presence of BSA, and indeed did not observe any significant changes (Supplemental Figure 1B).

These results indicate that the MC region on $Hsp90_{Ec}$ is sufficient to bind a large partially folded region of 131 .

The change in chemical shifts in the ^{15}N and ^1H dimensions are plotted across the 131 sequence in Figure 3B. The affected residues span the region (residues 80–115 on 131) that disappeared upon binding to full-length $Hsp90_{Ec}$. In native SN this binding region consists of the final strand of the β-barrel, β6, followed by a central helix, α2, followed by the loop connecting the C-terminal α3 helix (inset, Figure 3B). The residues showing large chemical shift changes (*e.g.* $\delta^{15}N > 0.2$) (D83, Y85, G86, Y91, I92, L103, V104, G107, V114) are primarily hydrophobic. A comparison the direction of these chemical shifts to average values for random coil, helix and strand (Supplemental Figure 2) suggests that the helical core and associated strands are preserved.

$Hsp90_{Ec}$ significantly alters the structure of 131

While the above measurements indicate which residues on 131 are involved in Hsp90 binding, they do not provide a clear picture of what kinds of conformational changes are taking place within 131 . Resolving this by NMR represents a major challenge due to 131 conformational heterogeneity. However, we reasoned that the ability of chemical crosslinkers to trap transient states combined with tandem mass spectrometry to identify the crosslinked sites, could provide these structural insights. That is, we will look for changes in intramolecular crosslinks that occur upon 131 binding to $Hsp90_{Ec}$ (see Methods). Analyzing the complex set of crosslinks is empowered by recent developments in bioinformatic tools for automatic analysis of LC-MS/MS data to identify crosslinked peptides [21; 22; 23; 24]. Crosslinks identified within $Hsp90_{Ec}$ alone confirm that the Cα of linked lysine residues are within the expected maximal distance of 24 Å (DSS length: 12 Å, lysine sidechain length: 6 Å). Of the 11 crosslinked lysines (Supplemental Table 1) all had Cα/Cα distances less than 20 Å (average: 14.1±4.3), indicating structural integrity of the complex under our cross-linking conditions.

Many intramolecular crosslinks were observed within 131 alone (31 total), consistent with its large number of lysine residues and its conformational flexibility. The relative abundance of each crosslink was quantified by ion intensity, with repeated measurements showing similar results (Supplemental Table 1). The 131 sample incubated with $Hsp90_{Ec}$ contained many of the same crosslinked lysine pairs, except a subset were significantly reduced (to <20% of peak intensity in the absence of $Hsp90_{Ec}$). As shown in Figure 4A the yield of 84:116 crosslink was the most reduced (95% reduction). Notably, this position spans the dominant binding region on 131 , suggesting that $Hsp90_{Ec}$ is specifically rearranging 131 structure. All ten of the most significantly reduced crosslinks involve at least one lysine residue within the $Hsp90_{Ec}$ binding region. The long-range nature of some of these destabilized contacts suggests that $Hsp90_{Ec}$ is also altering the 131 conformation distant from the immediate binding site. However, an alternative possibility could be that the change in crosslinks is reflecting a change in the global flexibility of 131 in the bound configuration.

In an effort to quantitatively interpret the crosslinking data, we used structural modeling. Briefly, about $9\cdot10^6$ coarse-grained Cα only conformations of 131 were generated with

varying levels of distance restraints to allow sampling of states ranging from fully unfolded to highly native-like. Since Δ131Δ exists in an ensemble of configurations, a combination of up to four structures was used to fit the crosslinking data. Including more than four states (for both the bound and free conformations) provided little improvement of the fit to the data. The modeled structures were scored by how they recapitulate the quantitative changes in crosslinking for all 31 lysine-lysine pairs (Supplemental Table 1). The result is a collection of structures that correspond to Δ131Δ alone and Δ131Δ upon interacting with $Hsp90_{Ec}$. The scores shown in Supplemental Figure 4A show how well different bound/free structure pairs describe the crosslinking data. For the top three scoring models, an accounting of how well they describe the crosslinking data is shown in Supplemental Figure 4B–D. Detailed structural examples of the top three scoring models are shown in Supplemental Figure 5.

The modeling approach appears to identify $Hsp90_{Ec}$-induced structural changes. For example, inspection of the top scoring structures immediately reveals that Δ131Δ undergoes an expansion upon binding to $Hsp90_{Ec}$ (Supplemental Figure 5). This structural rearrangement is evident in the top scoring pair of bound and free states (Figure 4B), with the increase in distance between residues 84 and 116 reflecting the observed loss of crosslinking in the bound state. A second observation from the modeling is that $Hsp90_{Ec}$ is opening the local conformation around the binding site on Δ131Δ. This opening is clear from a surface area analysis of the top three scoring models, shown in Supplemental Figure 6, which shows a significant increase in solvent accessible surface area at the interaction sites identified by chemical shift mapping (D83, Y85, G86, Y91, I92, L103, V104, G107, V114). The opening is most likely a direct consequence of these residues binding to $Hsp90_{Ec}$. While still qualitative, the modeling suggests that the chaperone competes for a specific set of hydrophobic contacts on the structured part of Δ131Δ; by interacting with these sites, the chaperone opens and remodels the surrounding substrate structure. Unfortunately, the lysine crosslinking information is too sparse, and the conformational variability too large, to make additional claims about identity of specific contacts between $Hsp90_{Ec}$ and Δ131Δ.

As an alternative, we used scanning cysteine crosslinking across both the hydrophobic and polar residues of the central amphipathic helix (Figure 5A) known to be critical for Δ131Δ binding to assess interactions with $Hsp90_{Ec}$. In the native state, the hydrophobic residues (M98, V99, A102, L103, V104) are relatively buried compared to the polar residues (K97, N100, E101, R105). Therefore, if $Hsp90_{Ec}$ has no effect of the structure of this region, it would be expected that crosslinking would preferentially occur at the exposed polar sites. In contrast, if $Hsp90_{Ec}$ is interacting with the hydrophobic face, and thus disrupting the local structure, then crosslinking would preferentially occur on the hydrophobic residues with a characteristic helical pattern.

As previous work had identified W467 on the Hsp90 middle domain as part of the Δ131Δ binding interface [18], we quantified cysteine crosslinking between a W467C mutant and each of the nine positions from 97–105 on Δ131Δ by integrating bands on a non-reducing gel. This clearly revealed a periodic pattern of crosslinking between $Hsp90_{Ec}$ and the hydrophobic face of the amphipathic helix (Figure 5B). The crosslinking saturated at a ~1:1

molecular stoichiometry (dimer $Hsp90_{Ec}$: 131). The crosslinking periodicity (two cycles over 9 residues) is close to that expected for two turns of an α-helix (7.2 residues). A modest level of mobility within the bound-state is suggested by the roughly equivalent crosslinking across that the hydrophobic face on 131 . Together the above findings show how hydrophobic contacts at Hsp90's flexible MD/CTD interface can bind to and reconfigure a partially folded substrate protein.

$Hsp90_{Ec}$ interacts with transiently populated unfolded states of native full-length SN

While Hsp90 is known to facilitate folding via handoff from Hsp70, many functions of Hsp90 are believed to result from its reconfiguration of native substrates. In principle Hsp90's recognition mechanism described above should work equally well in the folding and unfolding direction. While conventional binding studies failed to reveal interactions with full length native Staphylococcal Nuclease (SN) [17], it might be possible to detect interactions between $Hsp90_{Ec}$ and transient non-native states that exist within the full-length native SN ensemble. Although SN folding is cooperative, high energy partially folded states are sampled prior to complete unfolding [25; 26; 27]. Since hydrogen exchange (HX) can provide a very sensitive measure of the populations of such partially unfolded states, we used this approach to probe the ability of $Hsp90_{Ec}$ to alter the SN folding landscape.

A native SN HSQC shows that peak heights were uniformly decreased in response to increasing concentrations of $Hsp90_{Ec}$ (peaks offset for clarity, Supplemental Figure 7), similar to that observed with the p53 client [28]. Possible explanations include a weak native SN interaction with $Hsp90_{Ec}$ resulting in peak disappearance from slow tumbling and potential conformational changes, or interactions with a transiently populated SN state leading to higher populations of partially unfolded states and/or changes in folding dynamics. These possibilities can be separated by HX measurements with sub-stoichiometric quantities of $Hsp90_{Ec}$. Specifically, if $Hsp90_{Ec}$ is interacting with the native state of SN, then the HX rate should decrease and stoichiometric quantities of $Hsp90_{Ec}$ will be required to observe a significant effect. In contrast, if $Hsp90_{Ec}$ is interacting with unfolded states of SN, then only a limited chaperone concentration would be required for their stabilization, which would lead to increased HX that can be measured on the free SN population.

We first measured HX on SN in the absence of $Hsp90_{Ec}$. For full-length SN, many amide protons exchange upon dilution into D_2O within the dead-time of the first HSQC reflecting fast excursions around the native ensemble. The remaining amide protons show varying levels of exchange, as has been measured previously [25; 26; 27]. For example, residues 66 and 130 show significantly different exchange rates (Figure 6A blue squares) consistent with subglobal unfolding events exposing residue 130 before residue 66.

HX measurements in the presence of $Hsp90_{Ec}$ show a striking change in SN exchange rates. For example, position 66 has dramatically accelerated exchange whereas residue 130 is not significantly altered (black circles, Figure 6A). Only a sub-stoichiometric amount of $Hsp90_{Ec}$ (30 μM for 150 μM SN) is needed to observe this acceleration, indicating that the $Hsp90_{Ec}$ interaction is with a transiently populated partially folded state of SN. We used 30

μM as this is significantly above the Kd for binding 131   (~10 μM), thus any unfolded SN states can be readily bound by Hsp90$_{Ec}$.

We quantified the HX acceleration due to Hsp90$_{Ec}$ (Figure 6B), and found significant acceleration starting at residue ~20, becoming maximal between residues 60–80, and extending out to residue 100. There were no significant changes at the C-terminus of SN. Residues with HX acceleration greater than 10x are shown on the native SN structure in blue and residues with large chemical shifts or residues with significant cysteine crosslinking are shown in red (Figure 6C). These findings indicate that Hsp90$_{Ec}$ can dramatically enhance the probability of alternate conformations accessible within the native ensemble. However, since HX changes can occur both from stabilization of a non-native state as well as from a structural changes within a state, these measurements alone cannot demonstrate how Hsp90$_{Ec}$ affects folding intermediates.

Our HX measurements were performed at pH* 7.5, where SN is in the EX2 limit [25], which means that HX rates are governed by the equilibrium population of partially folded states that expose amide positions to bulk solvent. This means that many folding/unfolding events occur before HX happens, both in the presence and absence of Hsp90$_{Ec}$. The EX1/EX2 regime can be simply confirmed by measuring HX at a different pH, with EX2 behavior predicting uniformly faster exchange at higher pH, due to increased catalysis of HX by hydroxyl ions. Indeed, when we repeated the HX experiments at pH* 8.5 we found a similar fold acceleration of SN HX from Hsp90$_{Ec}$ with all the rates uniformly faster (data not shown). Given the EX2 regime, these measurements enable the free energy by which Hsp90$_{Ec}$ stabilizes non-native SN to be determined. The slowest exchanging residues in SN correspond to those exposed only during global unfolding [29]. Therefore, Hsp90$_{Ec}$-driven change in folding free energy can be calculated for a residue as

$\Delta\Delta G_{Hsp90} = -RTln(k_{SN}^{res}/k_{SN:Hsp90}^{res})$, which averages between 2–2.5 kcal/mol, depending on the reporting residue.

Discussion

Despite extensive research, it is not yet known how Hsp90 recognizes non-native states of its substrates and how the chaperone affects substrate structure and folding. Equally mysterious is how Hsp90 can facilitate protein-protein and protein-ligand interactions, behaviors that are associated with native folded proteins. Here we have used Hsp90$_{Ec}$ and a model substrate to investigate how Hsp90 recognizes and alters the structure of a partially folded target protein. We then demonstrate that Hsp90 can interact with non-native states of this substrate even in the context of a stable and fully native construct that only rarely samples non-native conformations. These findings provide the basis of a structural mechanism by which Hsp90 can alter the functional outcome of its substrates by binding and remodeling partially folded states that are transiently sampled from within the native ensemble.

The recent observation that the 131 -binding site on Hsp90$_{Ec}$ extends from the MD to the CTD [19] (Figure 1) immediately suggests that rearrangement of these domains allows the chaperone to adapt its structure to match potential binding sites on the substrate. Indeed, we showed here that by blocking Hsp90 conformational changes at the MD/CTD interface (via

the H446E mutation), 131 binding was dramatically reduced and the chaperone no longer undergoes substrate-driven conformational changes (Figure 2). Furthermore, the MD/CTD region alone is sufficient to recognize a large partially folded region of 131 (Figure 3). It is interesting to point out that a recent crystal structure of the closed state of the zebrafish mitochondria-specific Hsp90 (TRAP1) shows two distinct MD/CTD conformations [30]. One arm has a continuous hydrophobic surface, similar to the yeast crystal structure [6], whereas the other arm has an MD/CTD interface that is splayed out with the hydrophobic 131 interaction sites in a highly discontinuous surface. Consistent with our findings here, 131 binds to and activates the ATPase of human and zebrafish TRAP1, and binds better to the arm with the intact MD/CTD interface [30].

The dramatic defect in 131 binding from the H446E mutation provides a potential mechanistic explanation for functional defects observed in early Hsp90 genetic screens. Of four mutations in yeast Hsp90 that severely impaired nuclear receptor function [31] two were at the MD/CTD interface (T525I, A576T/R579K). One of the other mutations, E431K, is adjacent to a residue implicated in 131 binding (F390 in $Hsp90_{Ec}$, T433 in yeast Hsp90). Similarly, the CTD region of $Hsp90_{Ec}$ implicated in 131 binding has now also been implicated in the interaction of the ER Hsp90 (Grp94) with Toll-like receptors and integrins [32]. These observations are part of mounting evidence indicating that core features of the Hsp90 mechanism are universal among its diverse homologs. For example, the structural states of Hsp90 are conserved among homologs from divergent species but the population of these states are highly species-dependent [7]. Similarly, we propose that there are conserved features of substrate binding by Hsp90 while specific substrates may have additional modes of interaction tailored for specific needs.

The above observations suggest a mechanism of substrate recognition in which conformational changes at the MD/CTD allows the chaperone to recognize and adapt to specific, locally structured regions of the client that would normally be buried in the native state. A critical functional question is whether Hsp90 also significantly affects 131 structure and folding. Answering this has been a major experimental challenge, however important insights have come from a novel MS-crosslinking approach that focuses on changes in the pattern and abundance of 131 intramolecular crosslinks resulting from interaction with Hsp90 (Figure 4). Computational modeling of the crosslinking data suggests that $Hsp90_{Ec}$ is remodeling a previously buried hydrophobic cluster within 131 . Indeed, cysteine crosslinking confirmed that specific hydrophobic contacts are readily formed between Hsp90 and an amphipathic helix in 131 (Figure 5). These observations show that Hsp90 is capable of making significant structural alterations to specific regions in folding intermediates. Thus Hsp90 has the potential to reroute folding rather than just passively bind and release non-specific segments of protein chain.

A critical mechanistic distinction is whether Hsp90 only interacts with partially folded proteins when they are populated constitutively, as with 131 and during unfolding conditions, or whether Hsp90 can bind partially folded states that are only transiently sampled from a thermodynamically stable native state. The latter ability is directly supported by our observations on wild-type SN, for which no significant bulk binding is observed. First we found that $Hsp90_{Ec}$ reduces SN HSQC peak intensity, similar to observations made with

Hsp90 and p53 [28]. As with studies on p53, HSQC measurements alone were insufficient to determine if intensity loss was a consequence of a native interaction or an interaction with one or more partially folded states. However, we found that only a sub-stoichiometric concentration of Hsp90$_{Ec}$ was required for significant HX acceleration, demonstrating that Hsp90$_{Ec}$ stabilizes a low population partially folded state (Figure 6).

Given their modest stability, most proteins will fold and unfold many times during the lifetime of the protein, with many more partial unfolding events. Thus, the findings outlined above indicate that Hsp90 has the potential to alter the folding and activation fate of a client every time it partially unfolds. This in turn, could facilitate a client's ability to reach conformations relevant for interactions with ligands or other partners. This suggests that clients, such as kinases, could be recruited to the chaperone in the native state by co-chaperones, such as Cdc37, and that holding the client in proximity to Hsp90 would allow sufficient time for the client to sample a partially unfolded state, which then can be recognized and reconfigured by Hsp90. Further work with different clients is needed to test this proposed model.

Methods

Proteins were purified and isolated as descried previously [17; 18]. Binding measurements were performed on a Jobin Horiba fluorometer with IAEDANS-labeled Δ131Δ [17] and varying concentrations of Hsp90$_{Ec}$ or the H446E variant. The excitation/emission wavelengths were 340/480 and slit widths were both set to 5 nm, with an integration time of 1s. Small angle x-ray scattering was measured at the SIBYLS beamline (12.3.1) at the Advanced Light Source in Berkeley. Data was collected with 0.5, 2 and 5s integration times and buffer subtracted. The scattering data was analyzed with the GNOM program [33] and transformed to a P(r) representation.

NMR measurements were performed on a Bruker Avance 800. Isotopically labeled protein was expressed in M9 minimal media supplemented with 1g/L ^{15}N ammonium chloride and 0.5 g/L Isogro supplement (Sigma). Chemical shifts were measured with the ccpNMR software (http://www.ccpn.ac.uk). Random coil, helical, and strand chemical shifts were taken from the Biological Magnetic Resonance Bank (http://www.bmrb.wisc.edu). For HX experiments, native ^{15}N-labeled SN was concentrated to 1.5 mM and diluted 10-fold into D$_2$O, 25 mM TRIS pH* 7.5, 50 mM KCl, 10 mM MgCl$_2$, at 25 C, and successive HSQC measurements were recorded.

Scanning cysteine crosslinking was performed by incubating 50 μM of a Δ131Δ variant with 5 μM of W467C for 3 hours at room temperature with air oxidation, 25 mM TRIS pH 7.5, 50 mM KCl, 10 mM MgCl$_2$. Gels were imaged on a Kodak GelLogic 100, and band quantification was performed with ImageJ (http://rsbweb.nih.gov/ij/). The fractional degree of crosslinking was determined by integrating the area of the W467C monomer band (W), the W467C:Δ131Δ band (W:D), and then calculating W:D/(W+W:D).

For global lysine crosslinking, proteins were crosslinked with 5 fold molar excess of DSS (in 25 mM HEPES, 25 mM KCl, 5 mM MgCl$_2$, pH 8.5) at room temperature for 30 minutes.

To minimize the impact of the crosslinker on Hsp90 conformation, the chaperone was preclosed with AMPPNP. Previous work demonstrated that 131 can bind Hsp90$_{Ec}$ in the closed state [17]. Protein samples were separated by SDS-PAGE gel, in-gel digested and analyzed by LC-MS and LC-MS-MS as described previously [34]. The concentration of protein and crosslinker was optimized, so that only a small number of crosslinks per molecule would be formed and only specific crosslinks within the Hsp90/131 complex could be observed (Supplemental Figure 3). Briefly, an aliquot of the digestion mixture was injected into an Dionex Ultimate 3000 RSLCnano UHPLC system with an autosampler (Dionex Corporation, Sunnyvale, CA), and separated by a 75/25 cm PepMap RSLC column (100 Å, 2 μm) at a flow rate of 330 nl/min. The eluant was connected directly to a nanoelectrospray ionization source of an LTQ Orbitrap XL mass spectrometer (Thermo Scientific, Waltham, MA). LC-MS data were acquired in an information-dependent acquisition mode, cycling between a MS scan (m/z 315–2,000) acquired in the Orbitrap, followed by low-energy CID analysis on 3 most intense multiply charged precursors acquired in the linear ion trap. Activation time was 30 msec; automatic gain control targets were set at 200,000 for MS scans and 30,000 for MS/MS scans. Data was analyzed using an integrated bioinformatic workflow on the in-house version of the University of California San Francisco Protein Prospector (version 5.9.2), as described previously [21]. A precursor mass tolerance of 15 ppm and a fragment mass tolerance of 0.5 Da were used for protein database search. Cross-linked peptides were further inspected manually to assure correct identification.

To determine structural models corresponding to the lysine crosslinking data, we first defined a Bayesian scoring function, which is obtained from the posterior probability of having a model satisfying the cross-linking data and additional structural constraints. A full description of the theory is outlined in the Supplementary Information. The ensemble of bound and unbound 131 conformations that optimize the scoring function are organized into a parsimonious set of structures (a multi-state model with up to four states) that simultaneously explains the ratio of ion intensities crosslinked peptides (from Supplemental Table 1), native contacts (derived from HX data collected on SN, see below), basic secondary structure propensity (from SN crystal structure), and stereochemistry.

To create models with a range of structure, we used the foldon classification from native state HX of SN [25]. Foldons are defined as local substructures that hierarchically lose their native content along with the folding and unfolding reaction. The SN foldons are named by colors and in order of unfolding they are: *r*ed, *y*ellow, *g*reen, *b*lue. Therefore structures with all foldons used as constraints (*bgyr*) are more native-like and structures with only a subset of foldons (such as *bg*) have more structural freedom. We organized the modeling into a two step protocol: First, we generated, by sampling the posterior distribution, the most probable multi-state models given the binary cross-linking data. Second, we used the pool of generated models to best fit the quantitative cross-linking ratio data by enumerating all possible combination of models for the bound and unbound states. This analysis does not include the possibility of changes in crosslinking due to changes in lysine accessibility in the bound state (Supplementary Methods).

Supplementary Material

Refer to Web version on PubMed Central for supplementary material.

Acknowledgments

References

1. Haslbeck M, Franzmann T, Weinfurtner D, Buchner J. Some like it hot: the structure and function of small heat-shock proteins. Nat Struct Mol Biol. 2005; 12:842–6. [PubMed: 16205709]

2. Winter J, Ilbert M, Graf PC, Ozcelik D, Jakob U. Bleach activates a redox-regulated chaperone by oxidative protein unfolding. Cell. 2008; 135:691–701. [PubMed: 19013278]

3. Tapley TL, Franzmann TM, Chakraborty S, Jakob U, Bardwell JC. Protein refolding by pH-triggered chaperone binding and release. Proc Natl Acad Sci U S A. 2010; 107:1071–6. [PubMed: 20080625]

4. Krukenberg KA, Forster F, Rice LM, Sali A, Agard DA. Multiple conformations of E. coli Hsp90 in solution: insights into the conformational dynamics of Hsp90. Structure. 2008; 16:755–65. [PubMed: 18462680]

5. Krukenberg KA, Southworth DR, Street TO, Agard DA. pH-Dependent Conformational Changes in Bacterial Hsp90 Reveal a Grp94-Like Conformation at pH 6 That Is Highly Active in Suppression of Citrate Synthase Aggregation. J Mol Biol. 2009

6. Ali MM, Roe SM, Vaughan CK, Meyer P, Panaretou B, Piper PW, Prodromou C, Pearl LH. Crystal structure of an Hsp90-nucleotide-p23/Sba1 closed chaperone complex. Nature. 2006; 440:1013–7. [PubMed: 16625188]

7. Southworth DR, Agard DA. Species-dependent ensembles of conserved conformational states define the Hsp90 chaperone ATPase cycle. Mol Cell. 2008; 32:631–40. [PubMed: 19061638]

8. Krukenberg KA, Bottcher UM, Southworth DR, Agard DA. Grp94, the endoplasmic reticulum Hsp90, has a similar solution conformation to cytosolic Hsp90 in the absence of nucleotide. Protein Sci. 2009; 18:1815–27. [PubMed: 19554567]

9. Obermann WM, Sondermann H, Russo AA, Pavletich NP, Hartl FU. In vivo function of Hsp90 is dependent on ATP binding and ATP hydrolysis. J Cell Biol. 1998; 143:901–10. [PubMed: 9817749]

10. Panaretou B, Prodromou C, Roe SM, O'Brien R, Ladbury JE, Piper PW, Pearl LH. ATP binding and hydrolysis are essential to the function of the Hsp90 molecular chaperone in vivo. Embo J. 1998; 17:4829–36. [PubMed: 9707442]

11. Richter K, Soroka J, Skalniak L, Leskovar A, Hessling M, Reinstein J, Buchner J. Conserved conformational changes in the ATPase cycle of human Hsp90. J Biol Chem. 2008; 283:17757–65. [PubMed: 18400751]

12. Wayne N, Mishra P, Bolon DN. Hsp90 and client protein maturation. Methods Mol Biol. 2011; 787:33–44. [PubMed: 21898225]

13. Flanagan JM, Kataoka M, Shortle D, Engelman DM. Truncated staphylococcal nuclease is compact but disordered. Proc Natl Acad Sci U S A. 1992; 89:748–52. [PubMed: 1731350]

14. Alexandrescu AT, Abeygunawardana C, Shortle D. Structure and dynamics of a denatured 131-residue fragment of staphylococcal nuclease: a heteronuclear NMR study. Biochemistry. 1994; 33:1063–72. [PubMed: 8110737]

15. Wang Y, Shortle D. The equilibrium folding pathway of staphylococcal nuclease: identification of the most stable chain-chain interactions by NMR and CD spectroscopy. Biochemistry. 1995; 34:15895–905. [PubMed: 8519746]

16. Alexandrescu AT, Shortle D. Backbone dynamics of a highly disordered 131 residue fragment of staphylococcal nuclease. J Mol Biol. 1994; 242:527–46. [PubMed: 7932708]

17. Street TO, Lavery LA, Agard DA. Substrate binding drives large-scale conformational changes in the hsp90 molecular chaperone. Mol Cell. 2011; 42:96–105. [PubMed: 21474071]

18. Street TO, Lavery LA, Verba KA, Lee CT, Mayer MP, Agard DA. Cross-monomer substrate contacts reposition the Hsp90 N-terminal domain and prime the chaperone activity. J Mol Biol. 2012; 415:3–15. [PubMed: 22063096]

19. Genest O, Reidy M, Street TO, Hoskins JR, Camberg JL, Agard DA, Masison DC, Wickner S. Uncovering a region of heat shock protein 90 important for client binding in E. coli and chaperone function in yeast. Mol Cell. 2013; 49:464–73. [PubMed: 23260660]

20. Dollins DE, Warren JJ, Immormino RM, Gewirth DT. Structures of GRP94-nucleotide complexes reveal mechanistic differences between the hsp90 chaperones. Mol Cell. 2007; 28:41–56. [PubMed: 17936703]

21. Chu F, Baker PR, Burlingame AL, Chalkley RJ. Finding chimeras: a bioinformatics strategy for identification of cross-linked peptides. Mol Cell Proteomics. 2010; 9:25–31. [PubMed: 19809093]

22. Du X, Chowdhury SM, Manes NP, Wu S, Mayer MU, Adkins JN, Anderson GA, Smith RD. Xlink-identifier: an automated data analysis platform for confident identifications of chemically cross-linked peptides using tandem mass spectrometry. J Proteome Res. 2011; 10:923–31. [PubMed: 21175198]

23. Panchaud A, Singh P, Shaffer SA, Goodlett DR. xComb: a cross-linked peptide database approach to protein-protein interaction analysis. J Proteome Res. 2011; 9:2508–15.

24. Rinner O, Seebacher J, Walzthoeni T, Mueller LN, Beck M, Schmidt A, Mueller M, Aebersold R. Identification of cross-linked peptides from large sequence databases. Nat Methods. 2008; 5:315–8. [PubMed: 18327264]

25. Bedard S, Mayne LC, Peterson RW, Wand AJ, Englander SW. The foldon substructure of staphylococcal nuclease. J Mol Biol. 2008; 376:1142–54. [PubMed: 18201720]

26. Loh SN, Prehoda KE, Wang J, Markley JL. Hydrogen exchange in unligated and ligated staphylococcal nuclease. Biochemistry. 1993; 32:11022–8. [PubMed: 8218167]

27. Wrabl J, Shortle D. A model of the changes in denatured state structure underlying m value effects in staphylococcal nuclease. Nat Struct Biol. 1999; 6:876–83. [PubMed: 10467101]

28. Park SJ, Borin BN, Martinez-Yamout MA, Dyson HJ. The client protein p53 adopts a molten globule-like state in the presence of Hsp90. Nat Struct Mol Biol. 2011; 18:537–41. [PubMed: 21460846]

29. Huyghues-Despointes BM, Scholtz JM, Pace CN. Protein conformational stabilities can be determined from hydrogen exchange rates. Nat Struct Biol. 1999; 6:910–2. [PubMed: 10504722]

30. Lavery LA, Partridge JR, Ramelot TA, Elnatan D, Kennedy MA, Agard DA. Structural asymmetry in the closed state of mitochondrial Hsp90 (TRAP1) supports a two-step ATP hydrolysis mechanism. Mol Cell. 2014; 53:330–43. [PubMed: 24462206]

31. Bohen SP, Yamamoto KR. Isolation of Hsp90 mutants by screening for decreased steroid receptor function. Proc Natl Acad Sci U S A. 1993; 90:11424–8. [PubMed: 8248264]

32. Wu S, Hong F, Gewirth D, Guo B, Liu B, Li Z. The molecular chaperone gp96/GRP94 interacts with Toll-like receptors and integrins via its C-terminal hydrophobic domain. J Biol Chem. 2012; 287:6735–42. [PubMed: 22223641]

33. Svergun D. Mathematical models in small-angle scattering data analysis. J Appl Cryst. 1991; 24:485–492.

34. Chu F, Shan SO, Moustakas DT, Alber F, Egea PF, Stroud RM, Walter P, Burlingame AL. Unraveling the interface of signal recognition particle and its receptor by using chemical cross-linking and tandem mass spectrometry. Proc Natl Acad Sci U S A. 2004; 101:16454–9. [PubMed: 15546976]

35. Shiau AK, Harris SF, Southworth DR, Agard DA. Structural Analysis of E. coli hsp90 reveals dramatic nucleotide-dependent conformational rearrangements. Cell. 2006; 127:329–40. [PubMed: 17055434]

36. Creighton TE, Shortle D. Electrophoretic characterization of the denatured states of staphylococcal nuclease. J Mol Biol. 1994; 242:670–82. [PubMed: 7932723]
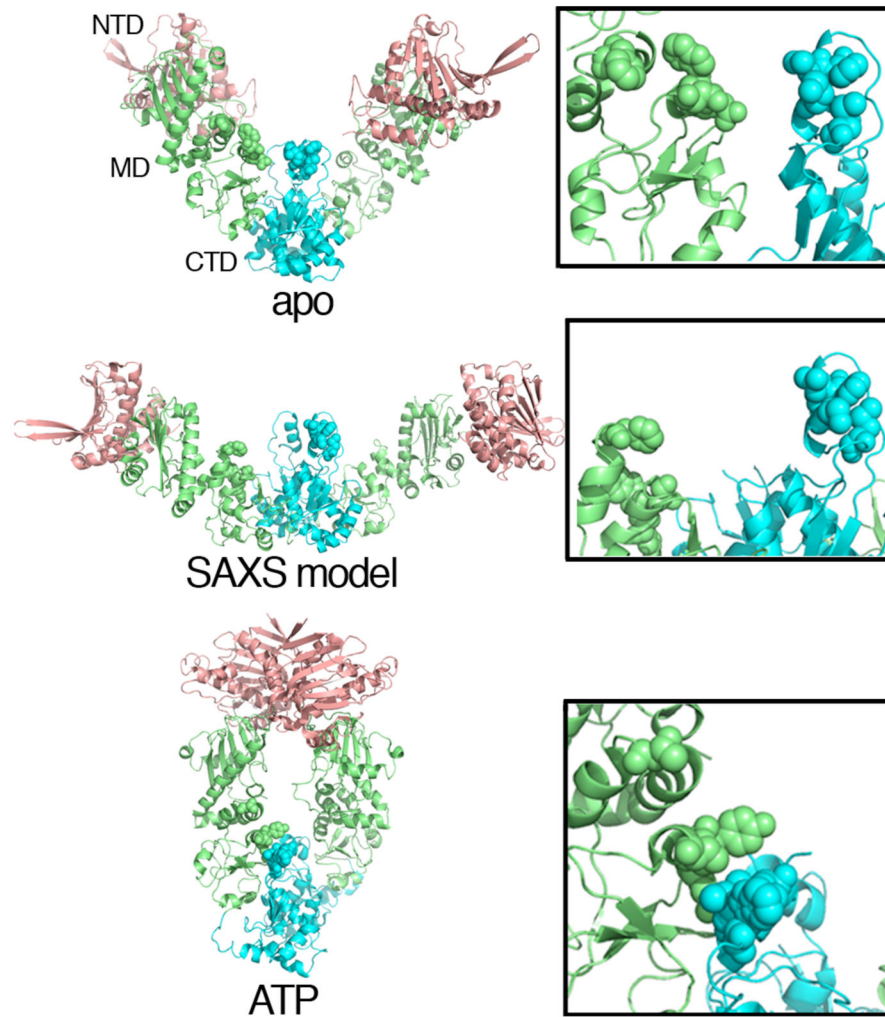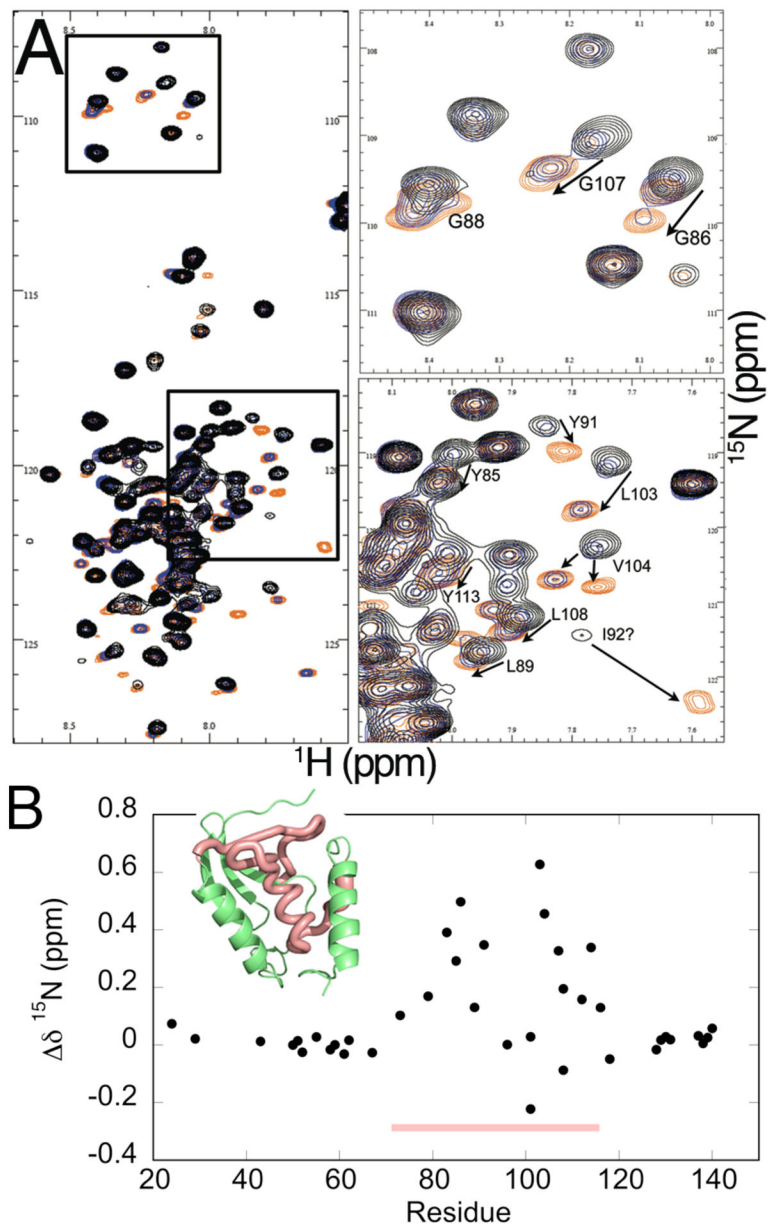
Figure 1.
(A) Hsp90 conformational heterogeneity is highlighted by dramatic conformational changes from nucleotide binding. Residues that significantly reduce 131 binding are shown in spheres at the MD/CTD interface. Positioning of these residues is significantly altered in the apo Hsp90$_{Ec}$ crystal structure [35], the SAXS model of the fully open state [8], and the closed state crystal structure of nucleotide-bound yeast Hsp90 [6].
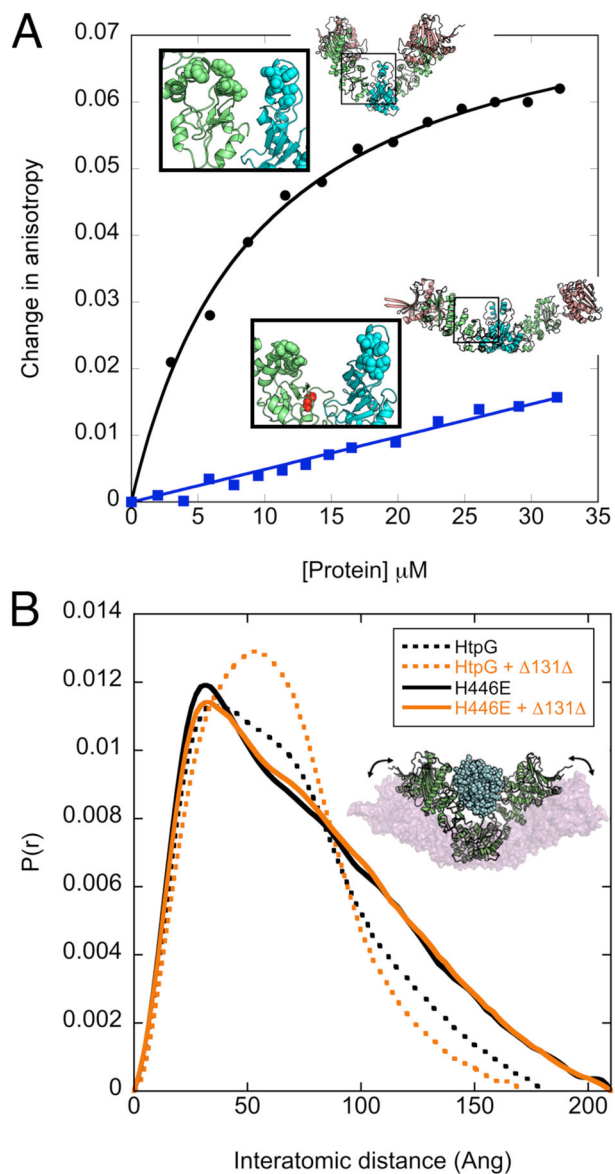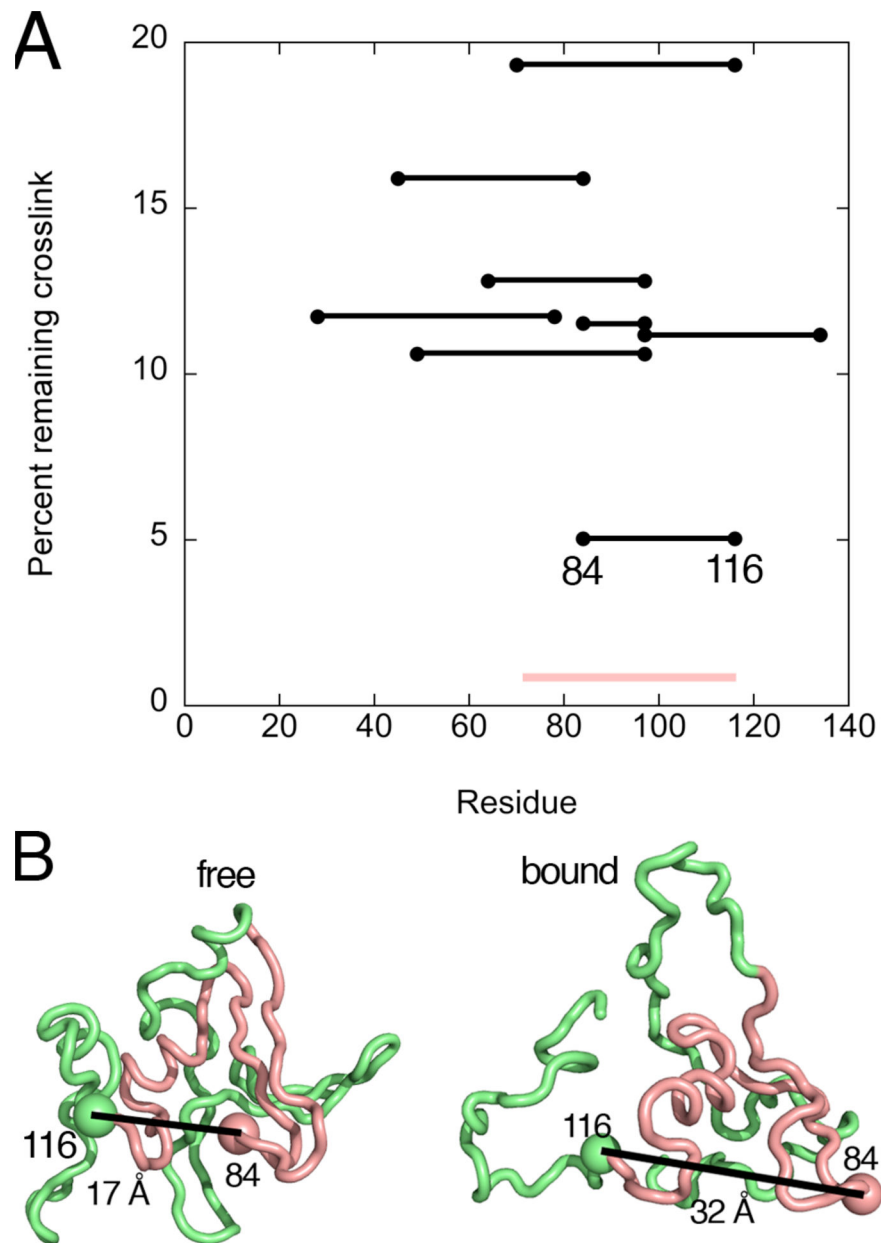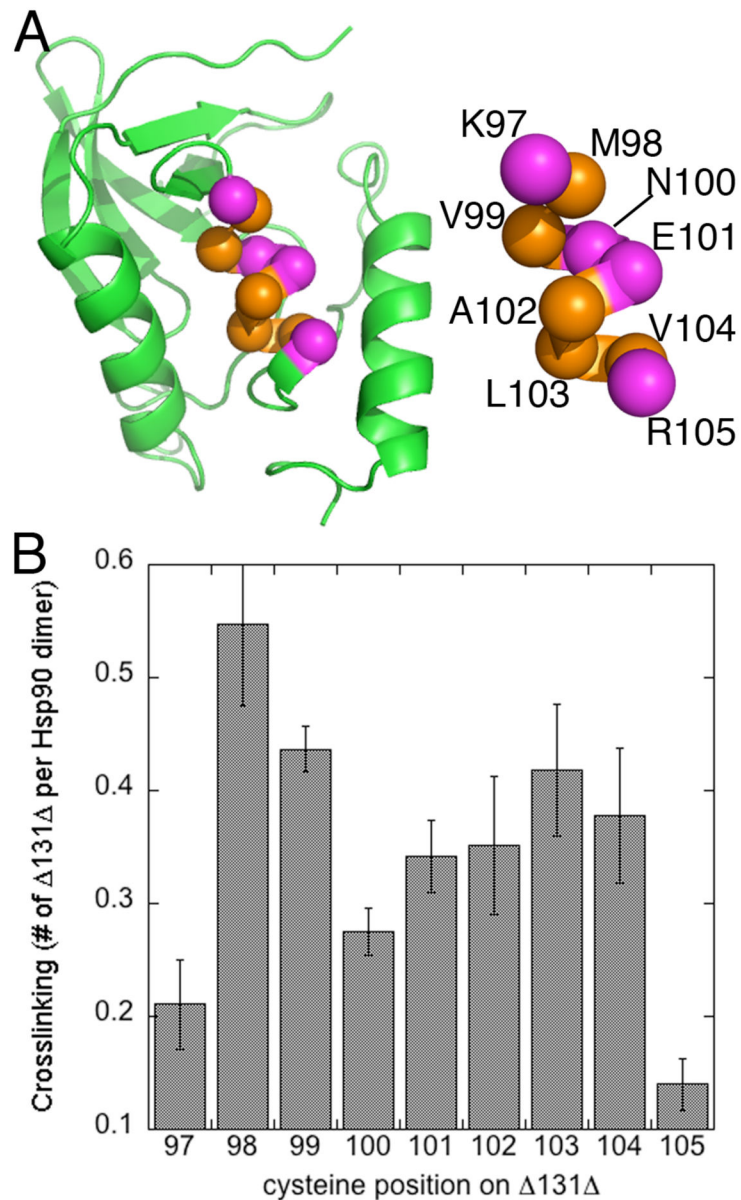
Figure 2.
(A) Binding measurements of Hsp90$_{Ec}$ (black circles) and the H446E variant (blue squares) show a dramatic difference in affinity for Δ131Δ. The insets show that the Δ131Δ binding region forms a continuous surface in the wild-type interface but in H446E this surface is broken. Position 446 is shown in red spheres. (B) SAXS measurements show that the conformation of Hsp90$_{Ec}$ is significantly altered by Δ131Δ[17], while the H446E variant is not significantly affected. Conditions: 25 mM TRIS pH 7.5, 25 mM KCl, 10 mM MgCl$_2$.
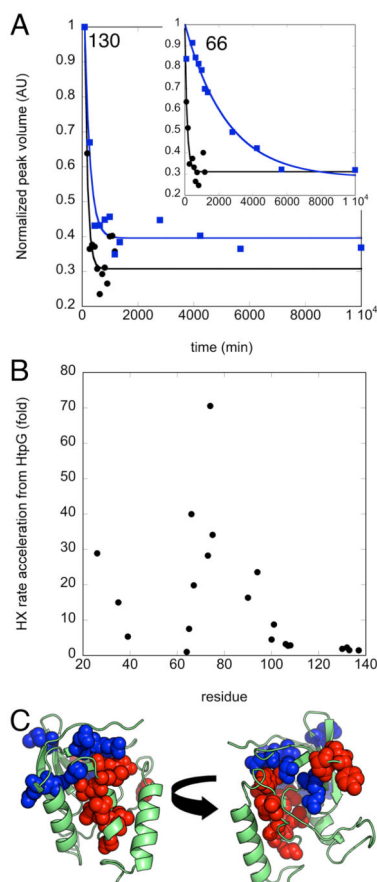
Figure 3.
(A) A 2D ^{15}N HSQC NMR spectrum of 131 alone (black contours) and with increasing concentrations of MC (blue and orange contours) shows a subset of residues affected by the interaction. (B) The chemical shift changes are plotted across the sequence of 131. Conditions: 25 mM MES pH 6.0, 75 mM KCl, 10 mM MgCl$_2$, 25° C, 150 µM 131 (black), 100 µM MC (blue), 300 µM MC (orange).

Figure 4.
(A) The changes in intramolecular Δ131Δ crosslinking due to Hsp90$_{Ec}$ are most evident in binding site identified by NMR. The crosslink most affected by Hsp90$_{Ec}$ spans residues 84:116 in Δ131Δ. (B) Modeling of the crosslinking data resulted in collections of bound and free structures. Structures from the top scoring model show a general expansion upon binding Hsp90$_{Ec}$, and associated exposure of the chaperone binding sites.

Figure 5.
(A) Residues tested in cysteine crosslinking are on the amphipathic helix in the center of the region of SN that binds to Hsp90$_{Ec}$. The helical pattern of hydrophobic residues is highlighted. (B) The degree of crosslinking across this portion of the Δ131Δ sequence shows a clear pattern in which contact with W467C is mediated by the hydrophobic face on this amphipathic helix.

Figure 6.
(A) HX kinetics of SN at positions 66 and 130 are shown in blue squares, highlighting an order of partial unfolding events in SN. Addition of a sub-stoichiometric concentration of Hsp90$_{Ec}$ leads to accelerated HX (black circles), although position 66 is significantly more accelerated than 130. (B) The HX acceleration from Hsp90$_{Ec}$ across SN shows that positions between 20–100 are significantly affected. (C) All sites with HX acceleration greater than 10x are colored in blue on the SN structure, while all contacting sites identified from chemical shifts and cysteine crosslinking are shown in red.